Shock and Vibration 18 (2011) 115–126
DOI 10.3233/SAV-2010-0580
IOS Press

Shaft crack identification based on vibration and AE signals

Wenxiu Lu* and Fulei Chu
Department of Precision Instruments, Tsinghua University, Beijing, 100084, P.R. China

Received 4 February 2010
Revised 2 June 2010

Abstract. The shaft crack is one of the main serious malfunctions that often occur in rotating machinery. However, it is difficult to locate the crack and determine the depth of the crack. In this paper, the acoustic emission (AE) signal and vibration response are used to diagnose the crack. The wavelet transform is applied to AE signal to decompose into a series of time-domain signals, each of which covers a specific octave frequency band. Then an improved union method based on threshold and cross-correlation method is applied to detect the location of the shaft crack. The finite element method is used to build the model of the cracked rotor, and the crack depth is identified by comparing the vibration response of experiment and simulation. The experimental results show that the AE signal is effective and convenient to locate the shaft crack, and the vibration signal is feasible to determine the depth of shaft crack.

Keywords: Shaft crack identification, acoustic emission, vibration, wavelet transform, cross-correlation, finite element method

1. Introduction

The shaft crack is a frequent and dangerous fault in rotating machinery. The expanding of crack may lead to the fracture of the shaft, which is a disaster for rotating machinery and causes great economic cost. It is very important and necessary to early detect and diagnose the shaft crack of rotating machinery timely and accurately, avoiding severe damage and expensive repairs.

A comprehensive research has been performed on the vibration of a cracked rotor system. Dimarogonas et al. [1] modeled a transverse surface crack as a local elasticity, which alters the elasticity of the whole cracked structure under consideration and related the crack depth with the decrease of the natural frequency. Dimarogonas et al. [2, 3] also developed a finite cracked Euler – Bernoulli element, and introduced the effect of coupling due to a crack expressed by a general local compliance matrix that had diagonal and non-diagonal terms. Sinou and Lees [4] analyzed the dynamic response of a rotor with transverse crack using the alternate frequency/time domain approach, and 2X harmonic components are observed at one-half of the first frequency, 3X at one-third of the first frequency. Bachschmid and Tanzi [5] presented a method to calculate the breathing behavior of transverse cracks of different types in rotating shafts including the thermal effects. Davies and Mayes [6] studied the effect of a propagating transverse crack on the dynamics of a rotor-bearing system using an experimental spin rig. They concluded that except for very large cracks, the vibration behavior is similar to that of a slotted shaft with additional excitation due to the crack opening and closing.

The vibration-based crack identification methods, especially the model-based methods, have been rapidly expanding over the last few years [7]. Seibold and Weinert [8] investigated detection techniques based on extended Kalman filters to detect the position and depth of crack whereby each filter represents a difference damage scenario.

*Corresponding author. Tel.: +86 10 62788308; Fax: +86 10 62788308; E-mail: luwenxiu@tsinghua.edu.cn.

ISSN 1070-9622/11/$27.50

Pennacchi and Bachschmid [9] presented a model-based transverse crack identification procedure in the frequency domain and applied to experimental results obtained on a medium size test rig. Three cases of crack identifications have been presented and the accurate results confirm the validity of the proposed approach. Sekhar [10] proposed a model-based method for the on-line identification of crack in a rotor, in which, the fault-induced change of the rotor system is taken into account by equivalent loads in the mathematical model and the nature and symptoms of the crack are ascertained using the fast Fourier Transform. Dong [11] presented a parameter identification method of a rotor with an open crack by using the first two natural frequencies and the first mode shape, in which the shaft is modeled as an Euler – Bernoulli beam without regard to the cross-section rotating inertia. Yu and Chu [12] used p-version of finite element method to estimate the transverse vibration characteristics of a cracked functionally graded material beam, and the frequency contours with respect to crack location and size are plotted and the intersection of contours from different modes indicates the predicted crack location and size.

However, the crack identification methods based on the vibration behavior of mechanical systems and structures are in general not sensitive to cracks of relatively small dimensions, in particular for detection during a regular exploitation of the real object. Acoustic emission technology is suitable technology to diagnose the crack fault. Acoustic emissions are defined as transient elastic waves generated from a rapid release of strain energy caused by a deformation or damage within or on the surface of a material [13], especially by the crack generation and expansion. Recent years, application of Acoustic emission technique has been growing in fault diagnostics of rotating machinery, especially in bearing defect diagnosis [14], rubbing fault location determination [15] and gear fault detection [16]. AE signal is often used to detect whether these faults occur and to determine where the faults occur, especially to determine the crack location [17,18]. Ghosal et al. [19] developed a Physics-Based Model (PBM) to provide a basic understanding of the actual physical process of asymmetric Lamb mode wave generation and propagation in a plate, which is very useful for the fault diagnosis.

The AE signal is prevalent nondestructive evaluation tool in which the sensors pick up the elastic waves generated due to micro-cracking in metals, and matrix cracking and fiber breakage in composites. The specific merits such as global monitoring capability and the passive nature of sensing make it a preferable technique for real-time monitoring. For rotating machinery, the micro-crack may be generated and expanded during operation, and then the AE signal can be obtained on-line. In this paper, the union diagnosis method based on vibration (including keyphase signal) and AE signals is proposed. The AE signals are used to identify the location of the shaft crack and a model-based method is applied to identify the depth of the crack. The experimental results show that the AE sign al is effective and convenient to locate the shaft crack, and the vibration signal is feasible to determine the depth of shaft crack.

2. Experimental set-up

The experimental rig is driven by a direct current shunt motor as shown in Fig. 1. The rotor speed can be adjusted from 0 to 10000 rpm rapidly by the voltage speed controller. The length of the experimental rig is 1200 mm, the width 108 mm and the height 135 mm. The mass of the rig is about 45 kg. The experimental setup consists of the rotor kit with two supports and some disks, and a set of data acquisition system including some eddy current transducers and AE sensors. The two bearings are oil film bearings and the length of the bearing house in axial direction is 25 mm. The diameter of the shaft is 9.5 mm with the length 500 mm. Any position along the shaft can be selected as bearing point.

The keyphasor is a closing sleeve with an axial slot and the keyphase signal is obtained by eddy current transducer. The AE sensors used for this experiment were broadband type sensors with a relative flat response in the region between 20 KHz and 200 KHz. The AE sensors are usually placed on the non-rotating member of machine, such as the bearing house or the pedestal. All the signals from sensors were pre-amplified, filtered, and connected directly to a commercial data acquisition card, where a sampling rate of 2 MHz per channel was used during the test. The AE signals caused by shaft crack will suffer severe attenuation before reaching the sensor and the output signal from the AE sensors was pre-amplified at 60 dB.

The transverse crack of the shaft is produced by wire cutting, with length 9.4 mm, width 0.2 mm and depth 4 mm as shown in Fig. 2. The crack is about 168 mm to the right bearing house, as shown in Fig. 3, $d_2 = 168$ mm.

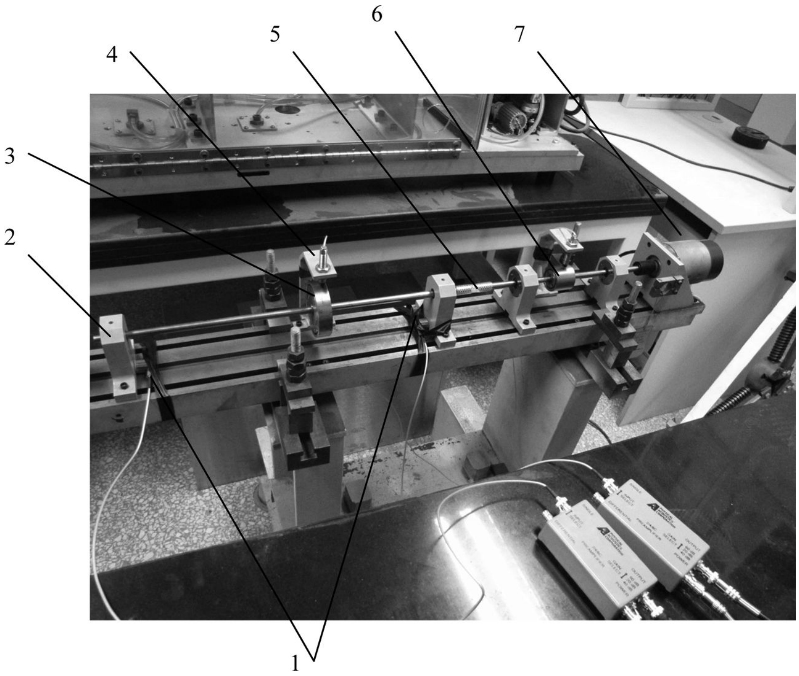

1. AE Sensor 2. Bearing house 3. Rotor 4. Eddy current transducer
5. Shaft coupling 6. Keyphasor 7. Motor

Fig. 1. Rotor rig.

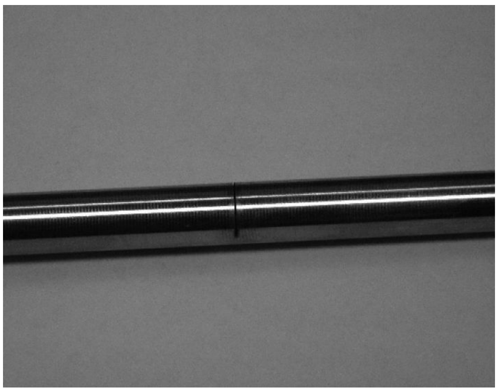

Fig. 2. Cracked shaft.

3. Crack location identification by AE signal

Using the differences in time-of-arrival from an AE source to two sensors, the position of the AE source can be simply calculated when the AE signal propagates along a constant-section shaft or beam. As shown in Fig. 3, the signals propagating from the AE source to bearing house A and B spend t_1 and t_2 time, respectively. In addition, propagating through oil film and bearing to Sensor A and B, spending t_3 and t_4 time. For different AE source at different position, t_3 and t_4 are the same. Then the gap Δt_{12} between t_1 and t_2 can be used to determine the position of AE source:

$$d_1 = \frac{l - V\Delta t_{12}}{2} = \frac{l - V(\Delta t + t_4 - t_3)}{2} \tag{1}$$

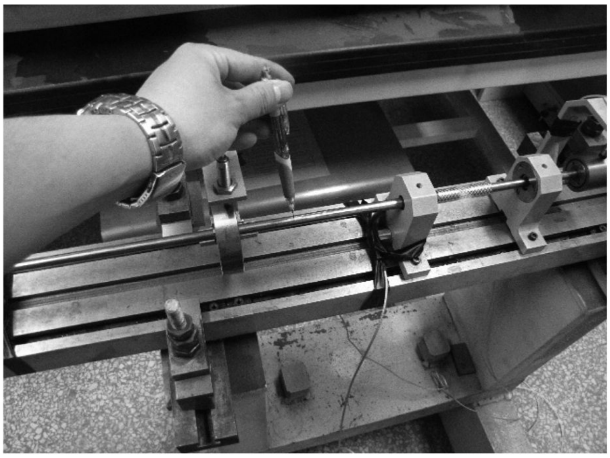

(a)

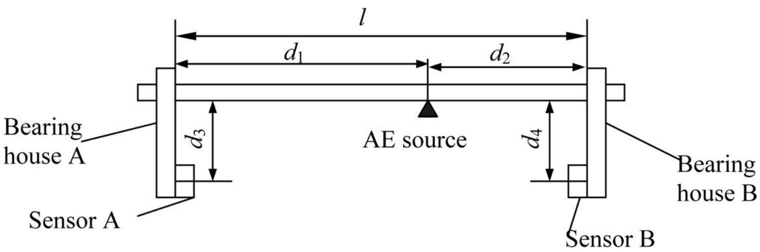

(b)

Fig. 3. Locating of AE source.

where d_1 is the distance between the AE source and sensor A, l is the distance between sensors A and B, V is the velocity of AE signal propagating in the shaft, and Δt is the gap between the arrival times of the two AE signals.

In Eq. (1), l can be measured directly with a value of 430 mm, and t_3, t_4 are constant in the rotor system. An important parameter is the propagation velocity V. The AE signal propagates along the shaft can be considered as longitudinal wave. The velocity for longitudinal wave in long rod is used:

$$V = \sqrt{\frac{E}{\rho}} \tag{2}$$

where E is Young's modulus, and ρ is the density of steel. Finally, V can be obtained as about 5200 m/s.

In order to determine the factual velocity V, t_3 and t_4, two pencil lead break tests were undertaken. One pencil lead break test was undertaken at position $d_1 = 252$ mm, the other $d_1 = 138.5$ mm. Then the last problem is how to calculate the time delay Δt between the two AE signals. In the past years, several approaches were used to determine the first arrival time. An amplitude threshold picker is the simplest one of them.

3.1. Threshold-based location method

Using the differences in time-of-arrival from an AE source to two sensors, the position of the AE source can be simply calculated. The traditional technology to detect time-of-arrival from AE source is the first time to cross the threshold. Figure 4 shows the waveforms of a pencil lead break AE signals from the bearing houses. Figure 4(a) shows the complete waveforms of AE signals when $d_1 = 252$ mm. It can be clearly seen that the amplitude of Sensor B is much larger than Sensor A, which indicates that the crack position is closer to Sensor B. The zoom waveform of AE signals is shown in Fig. 4(b), in which the delay time of the two signals can be observed clearly.

The threshold-based location method is very simple and fast, and can satisfy a certain error range, which leads to the wild applications in current AE detecting system. The insufficiency of this method is that the amplitude threshold

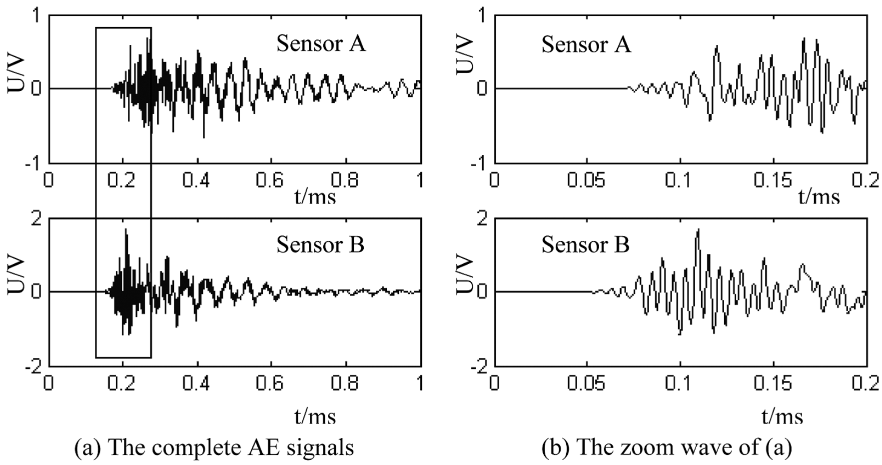

Fig. 4. The waveform of the pencil lead break AE signals.

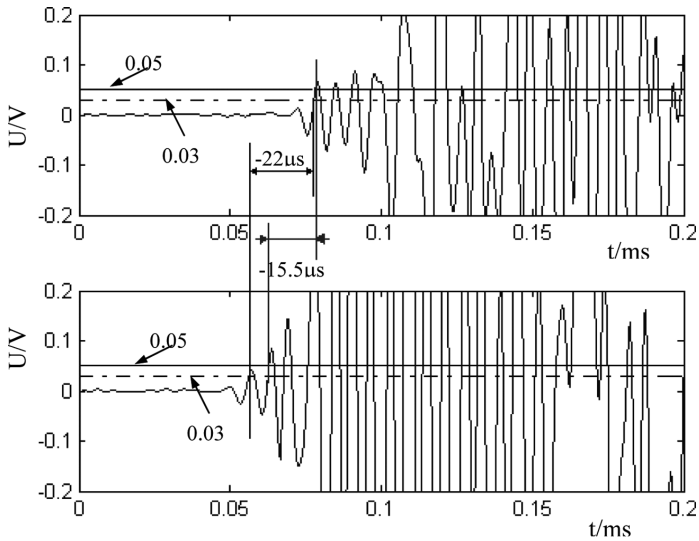

Fig. 5. The time delay by different threshold.

is preset by experience, which is not constant for different users. It may lead to different identification result. As shown in Fig. 5, when the amplitude threshold is set to 0.05, the delay time is -15.5 μs (right), while the amplitude threshold is set to 0.03, the delay time is -22 μs(wrong). Further more, the AE signal may be distorted along with the propagating path, especially dealing with low-amplitude signal or the signal with strong noise. Consequently, it may lead to a large location error and even to a false location.

3.2. Cross-correlation method

The cross-correlation is a conventional method for calculating the lag time between two signals. To compare the sampled data separately, the normalized cross-correlation coefficient ρ_{xy} is used as in

$$\rho_{xy}(\tau) = \frac{R_{xy}(\tau) - m_x m_y}{\sigma_x \sigma_y} \tag{3}$$

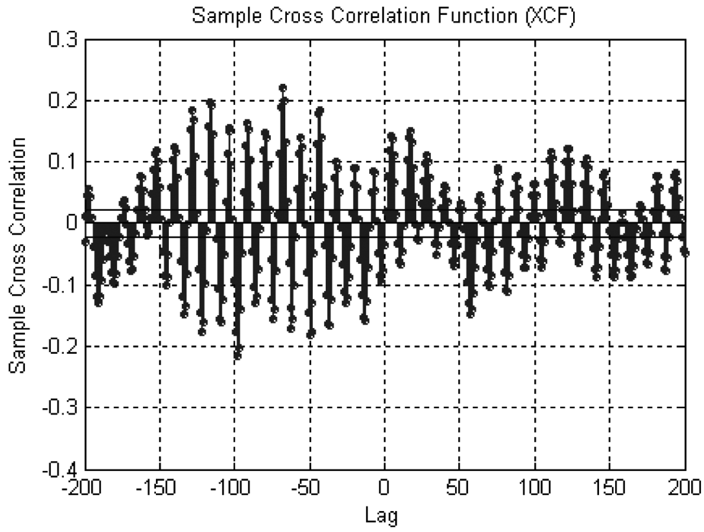

Fig. 6. The direct cross-correlation method.

Where $R_{xy}(\tau)$ is cross-correlation function, m_x and m_y are the mean values of the two signals respectively, σ_x and σ_y are the root mean square of the two signals respectively. When ρ_{xy} reaches its maximum value, the corresponding τ is Δt.

Though the cross-correlation is very useful in position pinpointing for cases such as structural defects, when it is applied directly to the cracked rotor system, it seems incapable. The structural characteristics of the rotor system are rather complex, which may influence the propagation of the AE signal. The influence of oil film on the propagation of AE signal is uncertain since the oil film can produce some AE signal. Actually, the form of the initial wave changes profoundly during propagation through the medium, and the signal emerging from the sensor has little resemblance to the original pulse. Therefore, the method of direct cross-correlation could be seldom to produce the right answer. Figure 6 shows that the max lags between the two AE signals. It can be calculated that $\Delta t = \Delta N/f_s = 68/2000000s = 34\mu s$, while the real Δt is about 15.5 μs.

The wavelet transform is very effective to improve the identification result [14]. Through wavelet transform, signals are decomposed into a series of time-domain signals, each of which covers a specific octave frequency band. The method of cross-correlation is applied to the decomposed signals to detect the AE source location.

Continuous wavelet transform (WT) of $x(t)$ can be defined as:

$$WT_x(a,\tau) = \frac{1}{\sqrt{a}} \int_{-\infty}^{+\infty} x(t)\psi^* \left(\frac{t-\tau}{a}\right) \mathrm{d}t, \quad a > 0 \tag{4}$$

Where $\psi(t)$ is the mother wavelet and the * indicates its complex conjugate. a and τ are real-valued parameters and can be used to characterize the scale and position features of wavelet. For the actual computation of the WT, a and τ should be dispersed. This is called discrete wavelet transform (DWT).

In the DWT, a signal can be represented by approximations and details. The approximation is the low frequency component of the signal. The detail is the high frequency component. In Fig. 7, 'S' represents the raw signal, 'A' represents the approximations and 'D' represents the details. A signal can be broken into lower-resolution components by using different scales. This is the wavelet decomposition tree.

When a signal is decomposed into j levels with DWT, there are totally $j+$ 1 wavelet components at level j as a result, i.e., in the frequency domain, $0 \sim f_{\max}$ is decomposed equally into

$$0 \sim \frac{1}{2^j} f_{\max}, \frac{1}{2^j} f_{\max} \sim \frac{1}{2^{j-1}} f_{\max}, \ldots, \frac{1}{2} f_{\max} \sim f_{\max} \tag{5}$$

DB5 wavelet is adopted to decompose the AE signal into 5 levels, and D5 signal is used for cross-correlation method. The result is shown in Fig. 8, in which the lag is -33 indicating the lag time Δt is -16.5 μs.

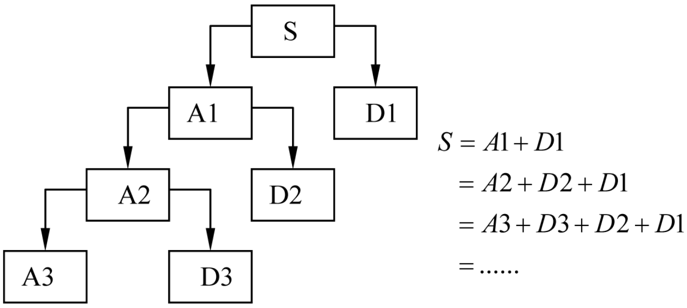

Fig. 7. Wavelet decomposition tree.

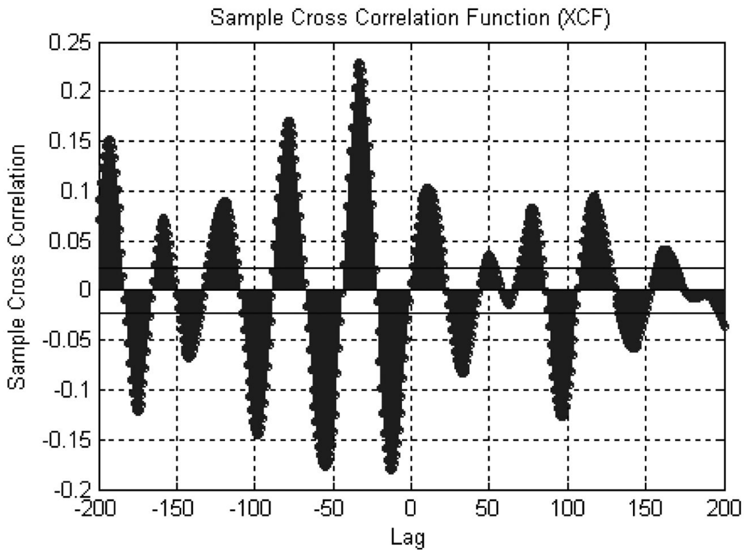

Fig. 8. The cross-correlation method based on wavelet transform.

The wavelet transform is effective in denoising and helps to improve the result of cross correlation. However, when the AE signals propagate in a complex structure, the wave reflection, wave refraction and wave mode conversion may occur when encountering various interfaces, which may lead to the wave attenuation and wave superposition. Consequently, the phase of a certain frequency or a certain frequency band signal may be changed during propagating, which may cause the cross-correlation location error even if after wavelet transform.

3.3. The improved union method

The AE signals are produced in the rotor system when the crack occurs and expands, and the elastic waves take the shortest path from the source to the sensors. The partial wave near the first time to cross the threshold is the fastest signal from the source to the sensors, which indicates that the partial wave is not or less influenced by the wave reflection and wave distorting. Using this partial wave to cross-correlation process may acquire an improved result. Then the improved union method can be express as following:

1. Applying the wavelet transform to the AE signal. Decomposing the signals into 5 levels and reconstructing the D5 signal.
2. Using the threshold-based location method to determine the approximate delay time of the two AE D5 signals and obtain the partial wave near the first time to cross the threshold..
3. Applying the cross-correlation method to the partial wave to amend the result of ii).

Table 1
The lag calculated by different method

Experiment No.	TM	DCM	WCM	TMW	TMWCM
1(d1 = 252mm)	−31	−68	−33	−28	−31
2(d1 = 252mm)	−31	−69	−66	−36	−29
3(d1 = 252mm)	−30	−84	−32	−24	−33
Average	−30.7	−73.7	−43.7	−29.3	−31
4(d1 = 138.5mm)	49	73	63	65	65
5(d1 = 138.5mm)	57	84	85	79	65
6(d1 = 138.5mm)	68	71	13	84	61
Average	58	76	53.7	76	63.7

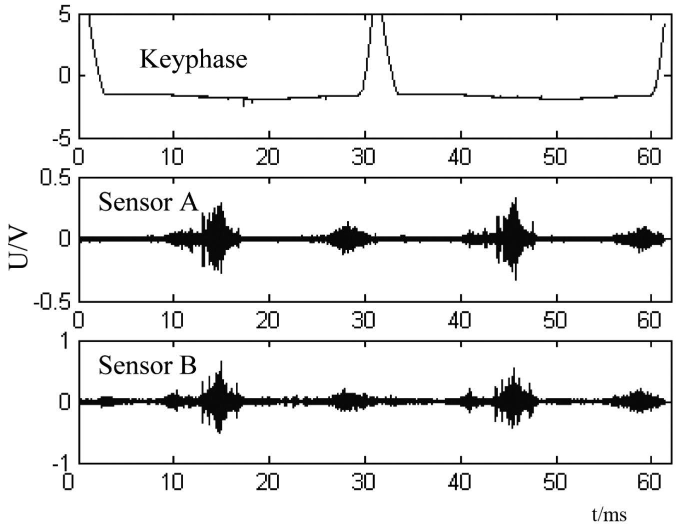

Fig. 9. Crack waveform at 2250 rpm.

3.4. Crack location identification

As described in Section 2, two pencil lead break tests were undertaken to determine the AE signal velocity V and $t_{3-}t_4$. Table 1 shows the result of identification of Δt using different method. TM represents threshold-based location method, DCM represents direct cross-correlation method, WCM is the wavelet transform cross-correlation method, TMW is the threshold-based location method after wavelet transform, TMWCM is the improved union method.

From the table, it can be seen that the identification result of DCM method and WCM method is not constant; while the identification result of TM is quite good if a suitable amplitude threshold is set; the best result is obtained by the TMWCM. From the result, it can be calculated $V =$ 4794.1 m/s and $t_{3-}t_4 =$ 0.055 μs.

For the shaft crack experiment, the crack is about 168 mm to Sensor B, that is, $d_1 =$ 262 mm. The first natural frequency of the system is around 44 Hz. The speed is increased to pass the first natural frequency till to about 3600 r/min, and then it is decreased to under the first natural frequency, last to still. The completely increasing and decreasing speed process is recorded for detail analysis. Figure 9 shows the keyphase signal and AE signal at bearing house. It can be seen that the AE energy mainly focuses on two regions per period and the phase of two regions are about 180°. Therefore, it can be concluded that the shaft crack is an open-close crack. During a whole period, when the crack is in open condition, the micro-cracks will be extended; while the crack is in close condition, the two sides of crack will impact each other slightly. Using the improved union method, Δt is equal to -18 μs, and $d_1 =$ 258.3 mm with an error ratio 1.41%.

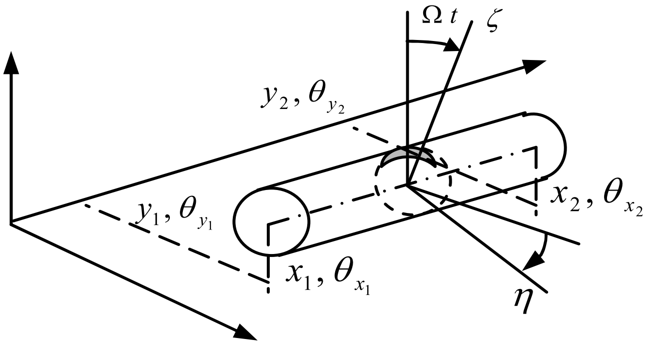

Fig. 10. Cracked shaft segment.

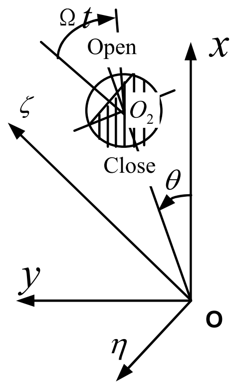

Fig. 11. Crack open-close condition.

4. Crack depth identification

4.1. Finite element model of cracked rotor system

The experimental kit is a rotor-bearing system with one disk and two supports, as shown in Fig. 1. The disk mass is 595 mg with imbalance mass 3g at radius 32.75 mm. The element model of the cracked system is established, and the cracked shaft segment is depicted in Fig. 10, and (x, y, z) is the fixed reference system. Thus, the finite element model equation can be obtained:

$$\mathbf{M}\ddot{U} + (\mathbf{G} + \mathbf{C})\dot{U} + (\mathbf{K_0} - \mathbf{K_c}(t))U = \mathbf{Q} \tag{6}$$

where *M*, *G*, *C* and K_0 are mass matrix, gyroscopic matrix, damping matrix, stiffness matrix, respectively. U is the vibration displacement vector including displacement and corner, Q is the excitation force including the imbalance force F_u, gravity force W, oil film force. K_c(t) is the stiffness decrease caused by the shaft crack.

Give the gravity force is much greater than the imbalance force, and then the crack is open and closed depending on the gravity force. Such crack open-close condition is shown in Fig. 11, where (ζ, η) is the rotational reference. In addition, the open-close function of the crack can be expressed as [7]:

$$f(\psi) = \frac{1 + \cos(\psi)}{2} \tag{7}$$

where $\psi = \Omega t - \theta + \pi$, θ is the related to the curvature of the shaft at the crack location and determined by the dynamic response of the shaft, $f(\psi) = 1$ denotes the crack is open while $f(\psi) = 0$ denotes the crack is close completely.

Assuming the maximal stiffness decrease caused by the crack is $\Delta k_\zeta, \Delta k_\eta$ in ζ, η directions, respectively. Then K_c(t) in the fixed reference system can be computed as following.

Table 2
FEM shaft segment parameters

Segment no.	(1)	(2)	(3)	(4)	(5)	(6)	(7)	(8)	(9)	(10)	(11)
Length [mm]	30	20	20	20	20	20	20	20	20	20	20
Segment no.	(12)	(13)	(14)	(15)	(16)	(17)	(18)	(19)	(20)	(21)	
Length [mm]	20	20	20	20	20	20	20	20	20	20	

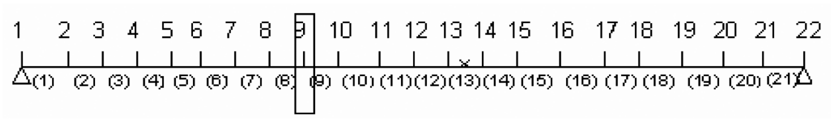

Fig. 12. Rotor kit FEM cell partition.

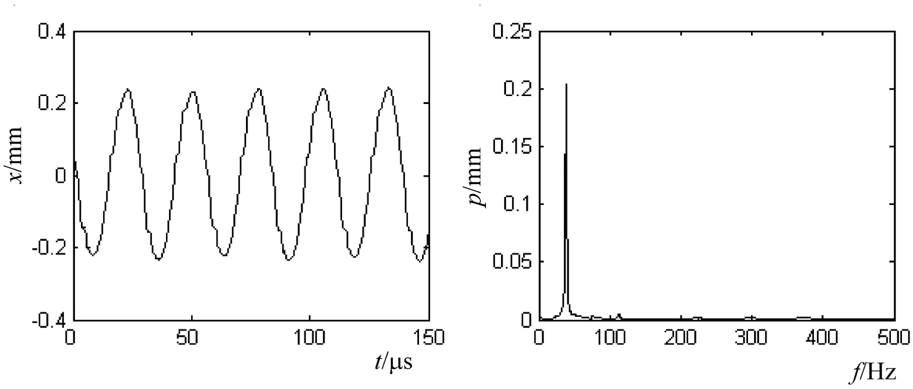

Fig. 13. The waveform and spectrum of cracked rotor.

$$\mathbf{K}_c(t) = f(\psi)\begin{bmatrix}\Delta k_\zeta \cos^2(\Omega t) + \Delta k_\eta \sin^2(\Omega t) & (\Delta k_\zeta - \Delta k_\eta)\sin(\Omega t)\cos(\Omega t) \\ (\Delta k_\zeta - \Delta k_\eta)\sin(\Omega t)\cos(\Omega t) & \Delta k_\zeta \sin^2(\Omega t) + \Delta k_\eta \cos^2(\Omega t)\end{bmatrix} \quad (8)$$

Dimarogonas and his colleagues [3] derived a rough analytical estimation of the local flexibility, which is a function of the relative crack depth a/D (a for crack depth, D for shaft diameter). From the flexibility matrix, $\Delta k_\zeta, \Delta k_\eta$ can be calculated.

Thus, the dynamic response of the rotor system can be obtained by nonlinear Newmark-β method.

4.2. Crack depth identification

After the finite element method (FEM) model of the cracked rotor is established with the crack depth as a fault parameter, the nonlinear dynamic response of the cracked rotor is obtained by Newmark method and compared with the experiment data, and then the parameter identification problem can be transferred into the optimization problem. A fitness value, which points out the approximate level to the optimal solution, is computed as the difference between the actual shaft vibration outputs at some points on the shaft and the computed results using FEM at fixed point on the shaft. In order to reduce the influence of the noise and keyphase in the sampling, the error in the frequency domain is used to compute the fitness function:

$$dif = 1 \Big/ \sum_{k=1}^{N/2} [(F_k - \bar{F}_k)^2] \quad (9)$$

where $\bar{F}_k$ is the frequency value of the sampled data, F_k is the computed frequency values of the computing result, N is the number of sample points.

The finite element model of the experimental rig is illustrated in Fig. 12 and the detailed parameters shown in Table 2. The cracked shaft segment is No.13 segment. Then the nonlinear dynamic response of the rotor system can be easily computed by Newmark-β method. The actual waveform and spectrum of cracked rotor at rotating speed 2220 rpm are shown in Fig. 13. It can be seen that the waveform is similar to sine wave, and there are a big 1X component in the spectrum. The 2X, 3X and some other higher harmonic components can be clearly observed in the spectrum.

Let a/D from 0 to 0.5 with step 0.01, the dynamic response of the rotor system are computed by nonlinear Newmark-β method. The minimal difference between the actual shaft vibration output at the disk and the computed result using FEM indicates the real crack depth. It can be easily identified that the a/D is 0.39, that is, a is 3.71 mm (The exact value is 4.0 mm). For real application, the result is acceptable.

5. Conclusions

In this paper, a methodology based on AE signal and vibration signal was presented to identify the shaft crack position and depth in rotor system. To detect the crack location with AE technique is a convenient and simple method. A higher accuracy of the location can be achieved by only using a higher sampling frequency. For the influences of oil film, structural characteristics, noise and other factors, the direct cross-correlation method and the amplitude threshold-based method do not give good result for detecting the crack location. Therefore, wavelet transform is applied to decompose the signal into a series of time-domain signals, each of which covers a specific octave frequency band. Then the threshold-based location method is used to determine the approximate location and the cross-correlation method to amend the identification result. The experiments have shown that this method is effective in improving the accuracy of the result. The finite element method is used to build the model of the cracked rotor system with the crack depth, and the depth is identified by the vibration signal in frequency domain. The experimental results show that the vibration signal is feasible to determine the depth of shaft crack.

Acknowledgements

This research is supported financially by National Natural Science Foundation of China (Grant No. 10702031, 10732060).

References

[1] T.C. Chondros and A.D. Dimarogonas, Identification of cracks in welded joints of complex structures, *Journal of Sound and Vibration* **69** (1980), 531–538.
[2] G. Gounaris and A.D. Dimarogonas, Finite element of a cracked prismatic beam in structural analysis, *Computers and Structures* **28** (1988), 309–313.
[3] C.A. Papadopoulos and A.D. Dimarogonas, Coupled longitudinal and bending vibrations of a rotating shaft with an open crack, *Journal of Sound and Vibration* **117** (1987), 81–93.
[4] J.J. Sinou and A.W. Lees, The influence of cracks in rotating shafts, *Journal of Sound and Vibration* **285** (2005), 1015–1037.
[5] N. Bachschmid and E. Tanzi, Vibration pattern related to transverse cracks in rotors, *Shock and Vibration* **9** (2002), 217–224.
[6] W.G.R. Davies and I.W. Mayes, The vibrational behavior of a multi-shaft, multi-bearing system in the presence of a propagating transverse crack, *Journal of Vibration, Acoustics, Stress, and Reliability in Design* **106** (1984), 146–153.
[7] S.W. Doebling, C.R. Farrar and M.B. Prime, A summary review of vibration-based damage identification, *Shock Vibration Digital* **30** (1998), 91–105.
[8] S. Seibold and K. Weinert, A time domain method for the localization of cracks in rotors, *Journal of Sound and Vibration* **195** (1996), 57–73.
[9] P. Pennacchi, N. Bachschmid, A. Vania, A model-based identification method of transverse cracks in rotating shafts suitable for industrial machines, *Mechanical Systems and Signal Processing* **20** (2006), 2112–2147.
[10] A.S. Sekhar, Crack identification in a rotor system: a model-based approach, *Journal of Sound and Vibration* **270** (2004), 887–920.
[11] G.M. Dong, J. Chen and J. Zou, Parameter identification of a rotor with an open crack, *European Journal of Mechanics, A/Solids* **23** (2004), 325–333.
[12] Z.G. Yu and F.L. Chu, Identification of crack in functionally graded material beams using the p-version of finite element method, *Journal of Sound and Vibration* **325** (2009), 69–84.
[13] J.R. Mathews, *Acoustic Emission*, Gordon and Breach Science Publishers Inc., New York, 1983.
[14] C. Li and S.Y. Li, Acoustic emission analysis for bearing condition monitoring, *Wear* **185** (1995), 67–74.

[15] Q. Wang and F. Chu, Experimental determination of the rubbing location by means of acoustic emission and wavelet transform, *Journal of Sound and Vibration* **248** (2001), 91-103.
[16] T. Toutountzakis, C. K. Tan, D. Mba, Application of acoustic emission to seeded gear fault detection, *NDT&E International* **38** (2005), 27–36.
[17] R. Gangadharan, G. Prasanna, M.R. Bhat et al., Acoustic emission source location and damage detection in a metallic structure using a graph-theory-based geodesic approach, *Smart Materials and Structures* **18** (2009), 1–12.
[18] P. Sedlak, Y. Hirose et al., New automatic localization technique of acoustic emission signals in thin metal plates, *Ultrasonics* **49** (2009), 254–262.
[19] A. Ghoshal, W.N. Martin et al., Simulation of asymmetric Lamb waves for sensing and actuation in plates, *Shock and Vibration* **12** (2005), 243–271.